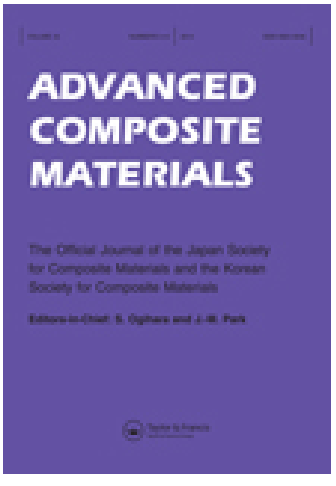

Advanced Composite Materials
Publication details, including instructions for authors and subscription information:
http://www.tandfonline.com/loi/tacm20

Mechanical properties of fiber/matrix interface in polymer matrix composites

Jun Koyanagi[a], Shinji Ogihara[b], Hayato Nakatani[c], Tomonaga Okabe[d] & Satoru Yoneyama[e]

[a] Department of Materials Science and Technology, Tokyo University of Science, Tokyo, Japan

[b] Department of Mechanical Engineering, Tokyo University of Science, Tokyo, Japan

[c] Department of Mechanical & Physical Engineering, Osaka City University, Osaka, Japan

[d] Department of Aerospace Engineering, Tohoku University, Sendai, Japan

[e] Department of Mechanical Engineering, Aoyama Gakuin University, Tokyo, Japan

Published online: 14 May 2014.

To cite this article: Jun Koyanagi, Shinji Ogihara, Hayato Nakatani, Tomonaga Okabe & Satoru Yoneyama (2014) Mechanical properties of fiber/matrix interface in polymer matrix composites, Advanced Composite Materials, 23:5-6, 551-570, DOI: 10.1080/09243046.2014.915125

To link to this article: http://dx.doi.org/10.1080/09243046.2014.915125

Advanced Composite Materials, 2014
Vol. 23, Nos. 5–6, 551–570, http://dx.doi.org/10.1080/09243046.2014.915125

REVIEW PAPER

Mechanical properties of fiber/matrix interface in polymer matrix composites

Jun Koyanagi[a]*, Shinji Ogihara[b], Hayato Nakatani[c], Tomonaga Okabe[d] and Satoru Yoneyama[e]

[a]*Department of Materials Science and Technology, Tokyo University of Science, Tokyo, Japan;* [b]*Department of Mechanical Engineering, Tokyo University of Science, Tokyo, Japan;* [c]*Department of Mechanical & Physical Engineering, Osaka City University, Osaka, Japan;* [d]*Department of Aerospace Engineering, Tohoku University, Sendai, Japan;* [e]*Department of Mechanical Engineering, Aoyama Gakuin University, Tokyo, Japan*

(*Received 3 February 2014; accepted 25 February 2014*)

This paper reviews the mechanical properties of interface adhesion between the fiber and matrix mainly by interpreting the authors' past articles. First, the methods for evaluating interface mechanical properties are described considering micromechanical testing using single-fiber composite specimens. In particular, the test-type dependence of the obtained interfacial strength is discussed, and this paper suggests that the cruciform specimen technique is an appropriate testing method. Then, this paper presents another way to obtain interface properties that is extracted from a bulk composite test. Moreover, the time and temperature dependence of the interface strength and the interface failure envelope under a combined stress state are described, respectively. Interface toughness is also discussed at the end of this paper, and it is implied that the value might be much lower than those presented in many conventional articles.

Keywords: interface mechanical properties; polymer matrix composites; time dependence; temperature dependence

1. Introduction

Nowadays, polymer matrix composites have become prevalent as their usages are widespread, e.g. a main structural material for modern air vehicles. In such a situation, the 'interface' strength, which is the adhesion between the reinforcing fiber and the polymer matrix, is still an issue to be solved for composite materials. One might suppose that a high adhesive strength would be sufficient, but this is not always the case. There might be a case where the composite performance decreases when the interface bonding strength is too high.[1,2] The author suggests a strong interface can lead a lot of simultaneous fiber failure under tensile load; even an inherently strong fiber fails simultaneously by a failure of neighboring weak fiber via strong interface, which causes the composite tensile strength to decrease.[1] Therefore, it is still very important to measure the interface mechanical properties precisely.

The procedures to obtain interface properties are roughly classified into two types. One utilizes micromechanical testing using single-fiber composite specimens,[3–26]

*Corresponding author. Email: koyanagi@rs.tus.ac.jp

and the other discusses the interface properties by extracting them from the bulk composite behavior.[27–35] The authors have implemented multiple experiments and simulations for the purpose of obtaining precise interface properties and have accumulated much knowledge so far. This paper reviews conventional articles regarding the interface mechanical properties up to the present and introduces several reports that discuss key points on interface property measurement. Section 2 discusses how to obtain the precise interface strength by micromechanical testing using single-fiber composite specimens. We discuss the failure envelope under a combined stress state assuming two types of failure criteria. Section 3 describes the procedure of how to obtain the interface strength mainly based on numerical analyses. Section 4 thoroughly discusses and clarifies the findings regarding interface strength and toughness. This paper also includes the time (strain rate) and temperature dependence of the interface properties. Finally, we conclude with an overview of the interfacial property characteristics in Section 5.

2. Micromechanical testing of single-fiber composite specimen

2.1. Overview

Micromechanical tests of a single-fiber composite specimen [3–26] can simply evaluate the interface strength as shown in Figure 1; these tests include the single-fiber pull-out test, micro-bond test, single-fiber fragmentation test, Brountman test, cruciform specimen test, etc. These photographs were taken by the present authors, who have performed multiple types of tests on single-fiber specimens. The present study insists that the cruciform specimen test [3–6] is a promising method for evaluating the interface strength because interface failure occurs from a uniform stress region, not from a part where a stress singularity exists. This makes the cruciform specimen test deterministically differ from the other tests. The cruciform specimen test was first implemented by Gundel et al. [3] and was then developed further by Tandon and Kim [4] and the authors.[5,6,18] These articles present the interfacial failure envelope under combined stresses obtained by a cruciform specimen test, in which the off-load axis is varied to create various normal/shear stress ratios. One of the authors' previous studies [5] solves the important problem of the unclear microscopic location of interfacial failure initiation by a novel method. For that study, the failure envelope still remained partially indeterminable considering the following aspects. The analysis performed assumes an elastic body. Assuming an elastic body may lead to misunderstanding with respect to interface stress when the stress level at the interface failure exceeds the range of elastic deformation of the matrix resins. Another unknown aspect was that the interface strength obtained by the cruciform specimen test has not been compared with that obtained from other tests on combined-stress failure envelopes.

On the other hand, the conventional works are classified into three groups: articles mainly presenting interfacial tensile strength,[3,4,6] articles involving a combined stress state of normal and shear,[4,5,7,18] and articles basically dealing with interfacial shear strength,[8–17,19–26] which has been the focus of most of our attention. It is worthy to note here that Zhandarov and Mader [8] and Piggott [9] reviewed in detail many other studies that have been conducted primarily on interfacial shear strength. Several of the methods for evaluating interfacial shear strength are compared,[8–13,25] including the fragmentation test, push-out test, pull-out test, and micro-bond method, and the test-type dependence of the obtained interface strength has been discussed. This discussion is very important because such comparisons can be effective proofs for

demonstrating that the evaluation methods are reasonable. Some articles, however, have indicated that the results depend on the test method, even though the material systems are identical in each article.[9–12] A typical discussion there focuses on shear stress, not a combined stress state. This might be a factor that causes the test-dependent differences. Note that implementing only one test is useful for a qualitative comparison; for example, interface strength has been evaluated by a micro-bond test even in recent articles.[14,15]

One of the authors' previous papers compares the interface strengths obtained by cruciform specimen tests with that obtained by a conventional single-fiber pull-out test.[18] The single-fiber pull-out test is a classical test as presented by Chua and Piggott [16], Beckert and Lauke [17], and Piggott [26]. The key point in the authors' study is the quasi-real modeling of the fiber entrance part, as shown in Figure 1(a).[18] There is a matrix cone along the fiber due to the wetting meniscus, as shown by analysis of the single-fiber pull-out test. During specimen preparation, the liquid-state resin is partially drawn along with the fiber at the fiber entrance due to surface tension, which is dominated by the wettability between the fiber and resin. Since the specimen is cured as is, the cured specimen has a resin cone at the fiber entrance. We refer to this as the resin meniscus. The meniscus significantly mitigates any stress singularity and enables the calculation of the actual interface strength. In the following section, we introduce the results of the authors' study.[18]

2.2. *Single-fiber pull-out test considering resin meniscus*

We implemented single-fiber pull-out tests for two kinds of composite systems, the difference of which is the cure temperature used when preparing the specimen. Both specimens consist of a glass fiber and epoxy resin, but one is cured at room temperature, and the other is cured at 100 °C. The interface strength of the former is less than that of the latter [18]. Figure 2 shows the relationship between the pull-out load and fiber-embedded length and the apparent interfacial shear strength, which is obtained by dividing the pull-out load by the interface failure area, which is one of the most typical evaluation methods. As shown in Figure 2(b), the apparent interfacial shear strength is fiber-embedded-length dependent. We cannot determine which value is the exact interface strength; this tendency is consistent with those of many conventional methods.

The authors considered the resin meniscus, as shown in Figure 3. Comparing it with the photograph of the actual specimen shown in Figure 1(a), the modeling seems to be reasonable. The size of the meniscus differs, so we assumed the radius of the meniscus to be between 25 and 35 μm, which covers the scattering of each meniscus size. Furthermore, an inelastic constitutive equation is used for the matrix resin, which is based on the total strain theory.[36] Even though the analysis is not of the incremental type, considering the inelastic constitutive equation allows us to obtain a much more precise stress value than the elastic assumption at a relatively high stress state. The pull-out load at failure is set as a boundary condition. Figure 4 shows the stress distributions when assuming resin meniscus sizes of (a) 25 μm and (b) 35 μm (room temperature cured specimen, 0.112 N of load, 0.25 mm fiber embedded length). Note that non-negligible normal stresses exist. We take the maximum value as the interface failure combined stress state, and then Figure 5 can be derived from Figure 2(a). Apart from Figure 2(b), the interface failure combined stresses are not fiber-embedded-length dependent. This suggests that these values are intrinsic the interface strength (combined stresses at interface failure). The results are compared with those obtained from the

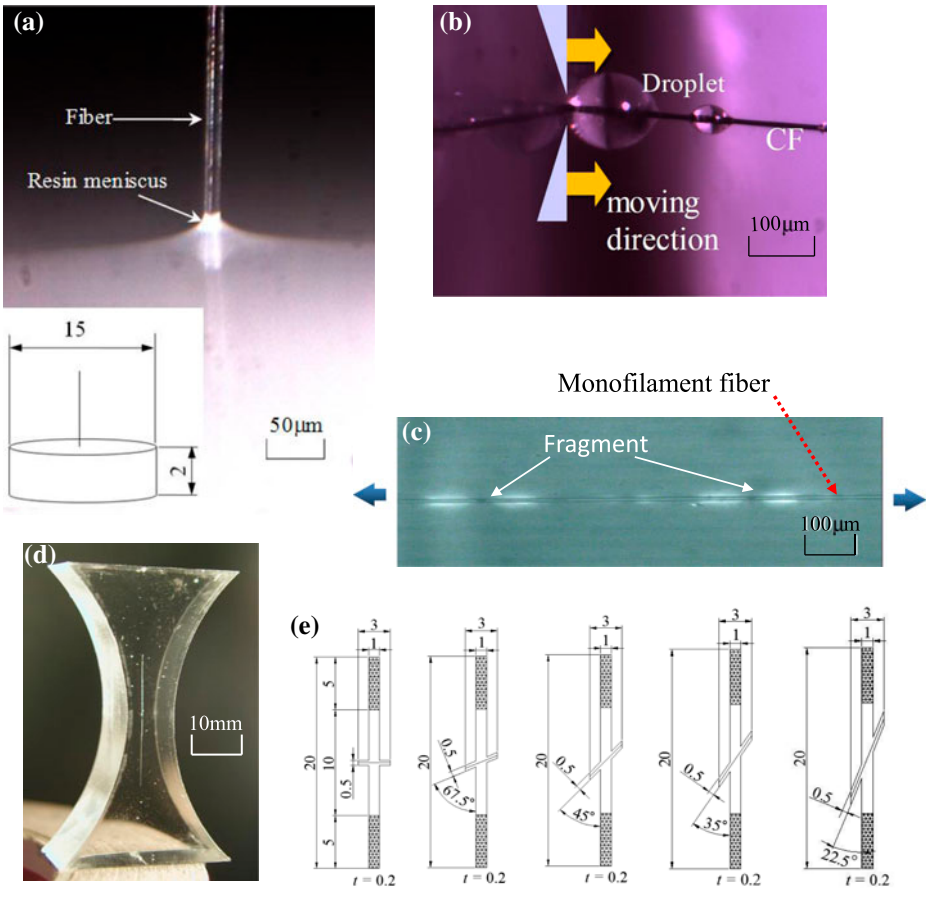

Figure 1. Photographs of specimens for various micromechanical testing: (a) single-fiber pull-out test,[18] (b) microbond test, (c) single-fiber fragmentation test, (d) Broutman test, (e) cruciform specimen test.[5]

cruciform specimen test in Figure 6. These are consistent with each other in terms of the interfacial failure envelope.

Thus, considering the meniscus and the inelastic constitutive equation, we can obtain an interface strength from the single-fiber pull-out test identical to those obtained from the cruciform specimen test. Only taking the maximum stress criterion, we can obtain identical interface strengths using several types of tests.

2.3. *Time and temperature dependence of interface strength*

Figure 7 shows the relationship between the interfacial normal strength measured using the cruciform specimen method and the test temperature presented in one of the authors' papers.[6] In this figure, 'Measurement limitation' relates to the epoxy resin strength as a function of temperature. This means we cannot obtain experimental results beyond this limitation because the specimen itself fails in advance of interface failure.

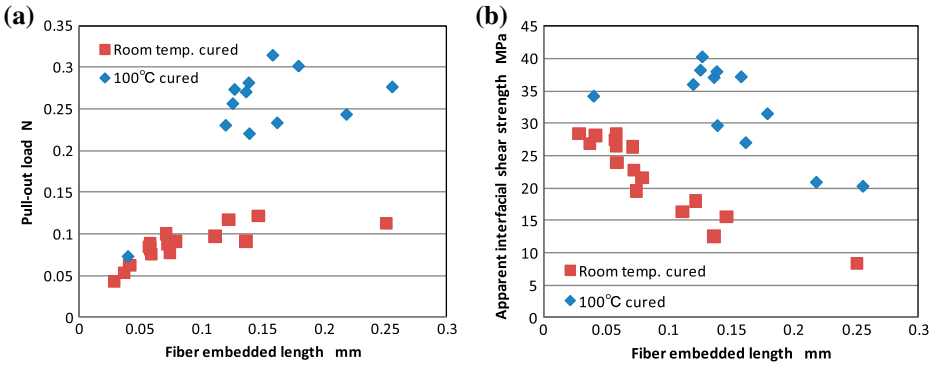

Figure 2. Single-fiber pull-out test results (a) pull-out load vs. fiber embedded length, (b) apparent interface shear strength vs. fiber embedded length.[18] Apparent interfacial shear strength which is the value of pull-out load divided by failure interface area decreases with increase of fiber-embedded length.

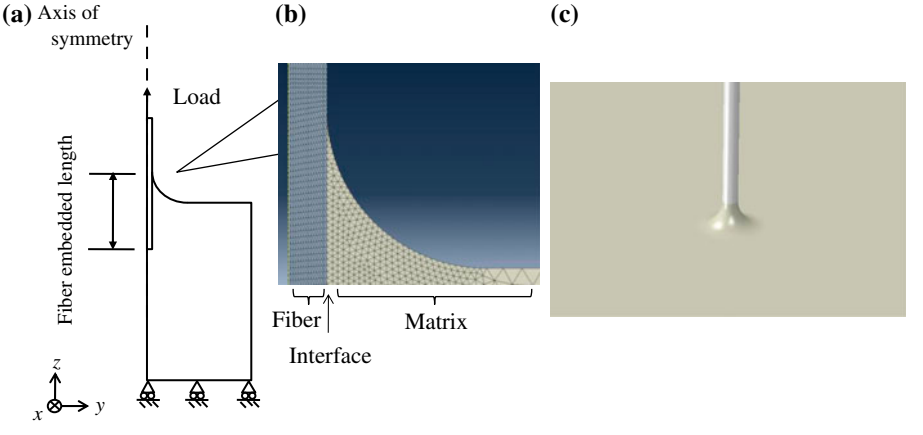

Figure 3. Schematic of FEA modeling: (a) Schematic of boundary condition, (b) mesh neighboring resin meniscus and definition of meniscus radius, R_m, (c) 3D views of resin meniscus modeling, $R_m = 30$ mm.[18] The resin meniscus modeling looks similar to actual specimen in Figure 1(a).

The interface strength seems to decrease with an increase in test temperature. However, considering the fact that experimental plots over the limitation cannot be obtained, i.e., even if there were a relatively strong interface, it does not appear in the experimental results that the two right-hand-side averages (50 and 60 °C) would be inherently larger than they are. Hence, the paper concludes that the interfacial normal strength is temperature independent.[6] Similarly, for our other results, which will be introduced in the following section, the interfacial normal strength is time and temperature independent. In contrast, Staub et al. [20] presented that the interfacial shear strength is temperature dependent via a microbond test. Further, one of the authors' papers [19] showed that the interfacial shear strength is time dependent using a single-fiber fragmentation test.

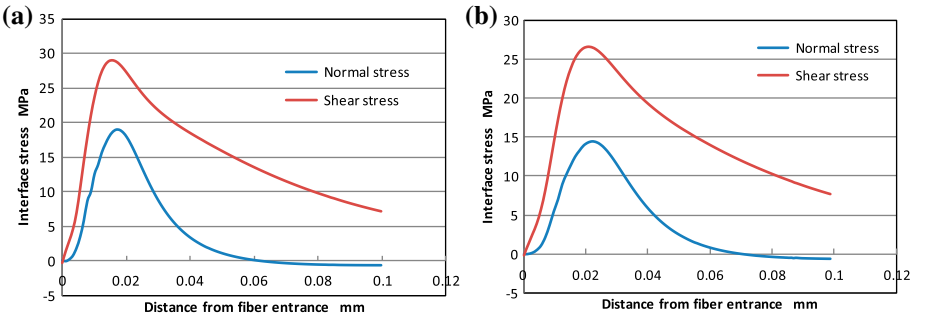

Figure 4. Interface stress distributions along with fiber, assuming (a) 25 μm, (b) 35 μm R_m.[18] (Room temp. cured specimen, 0.112 N of load, 0.25 mm fiber-embedded length) The stress values are not so drastically affected by size of resin meniscus in this range. The locations of maximum shear and normal stresses are near. Although pull-out test is supposed to be shear strength measurement test, not negligible normal stress exists at the failure initiation points.

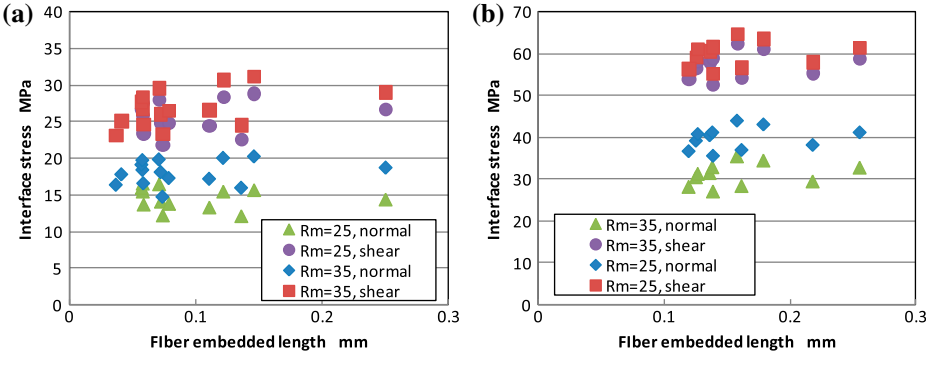

Figure 5. Fiber embedded length vs. normal and shear stresses at failure initiation point when interface fails for (a) room-temperature-cured and (b) 100 °C cured specimen.[18] There values are independent on fiber-embedded length; this means these stress combinations are actual interface strength.

When all of the above results are assumed to be correct, it is reasonable to consider a 'parabolic criterion' for the interface failure envelope.

Figure 8 shows the interface failure envelopes assuming the quadratic criterion and parabolic criterion. These two failure criteria are considered in Figure 6 as well. They do not significantly differ from each other when tensile and shear stresses are applied; however, when shear and compressive stresses exist, they obviously differ. In other words, in the parabolic criterion, existence of the compressive stress enhances the shear strength. The compressive stress can vary with time and temperature so that the interface shear strength also varies simultaneously. Consequently, in the case of a compressive and shear stress state, even if the interface failure envelope is not time and temperature dependent, the shear strength looks to be time and temperature dependent because the enhancement from the compressive stress can be time and temperature dependent. In one of the authors' papers,[19] time-dependent interface debonding propagation is numerically simulated using cohesive zone modeling to describe interface

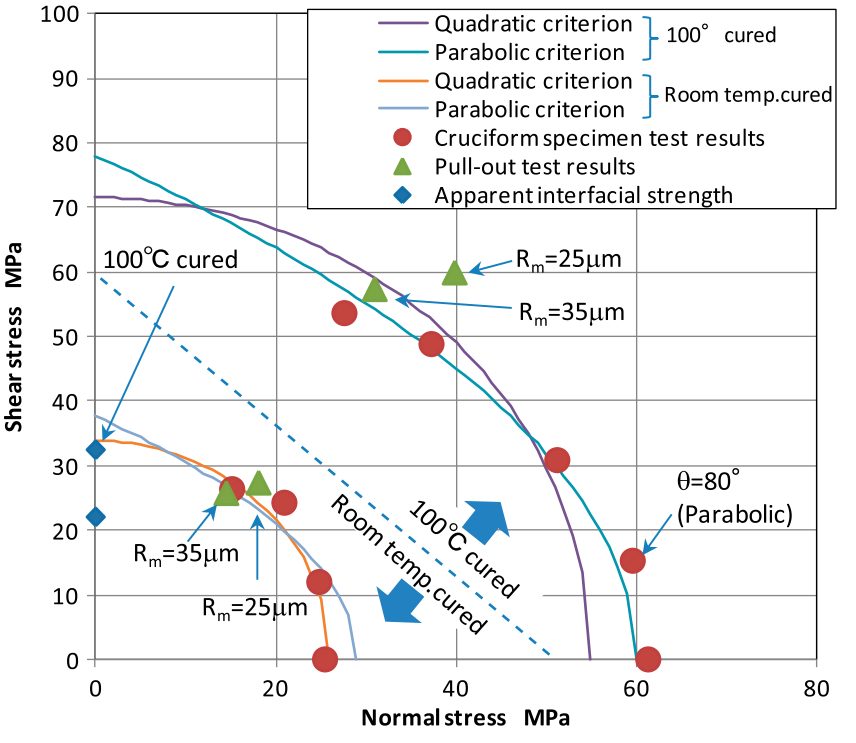

Figure 6. Interface failure envelopes assuming quadratic and parabolic criteria for room temperature cured and 100 °C cured specimens, based on cruciform specimen test and single-fiber pull-out test. The test results obtained from different tests are consistent each other.

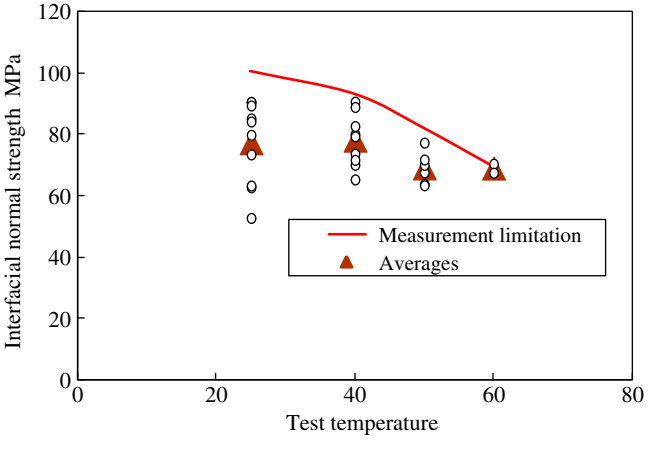

Figure 7. Interfacial normal strength vs. test temperature and measurement limitation.[6] At relatively high temperature tests, the specimen itself often fails in advance of interface failure so that it the interface strength is relatively high, the strength is not measured. The actual average values for them should be upper little more.

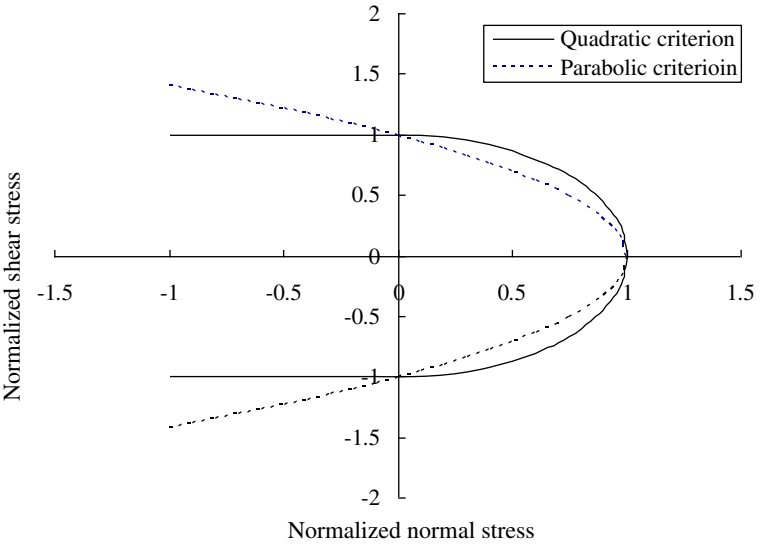

Figure 8. Interface failure envelope depicted on normalized normal and shear stresses field: quadratic criterion and parabolic criterion. In parabolic criterion, when compressive stress exists, interfacial shear strength is enhanced.

debonding, in which the interface properties are not time dependent, but the interfacial shear strength enhancement from the compressive stress is modeled. The numerical results match the experimental results very well. Thus, taking the parabolic criterion for the interface failure envelope, all of the above results can be explained consistently. Let us emphasize here that the interface strength is basically time and temperature independent.

3. Evaluation of interface properties using bulk specimen

3.1. Simple estimation of interface strength

The interface strength can be roughly estimated from a transverse tensile test of a unidirectional composite bulk specimen with the scheme presented by Ha et al. [28]. The article presented that when the critical point stress in a unit cell consisting of one fiber and the surrounding matrix resin, as shown in Figure 9, reaches either the matrix strength or the interface strength, the unidirectional composite fails by transverse loading. By observation of the failure surface, we can identify whether the composite failed by an interface-failure dominant mode or a matrix-failure dominant mode, as shown in Figure 10. For the case of an interface-failure dominant mode, the critical point stress corresponds to the interface normal strength. This procedure might not lead to a precise interface strength, but it is sufficient for a qualitative discussion of the interface strength.

The authors investigated the time and temperature dependence of the interface strength based on the abovementioned procedure.[27,35] A simple tensile test was performed at various strain rates and temperatures. Typical results for the failure surfaces are shown in Figure 10. At a high temperature and a low strain rate, the specimen tended to fail in the matrix-failure dominant mode. Under the opposite condition, the

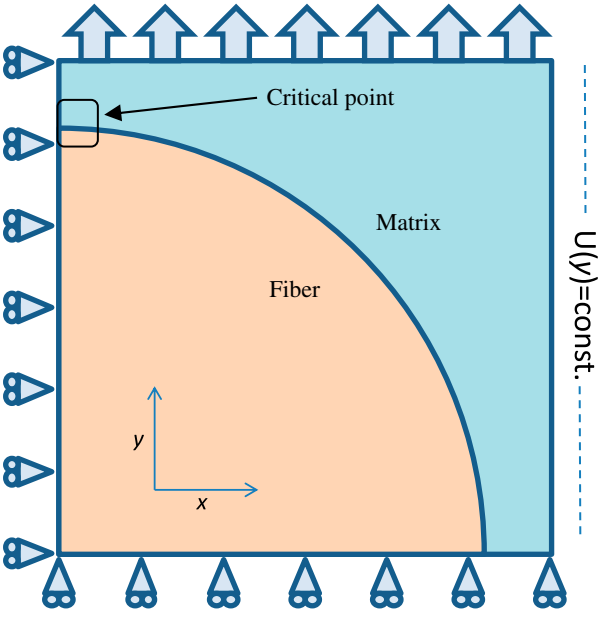

Figure 9. Schematic of the most simple unit cell for transverse tensile of unidirectional composite. The x displacements on the right-hand edge are the same. This model does not consider any damage.

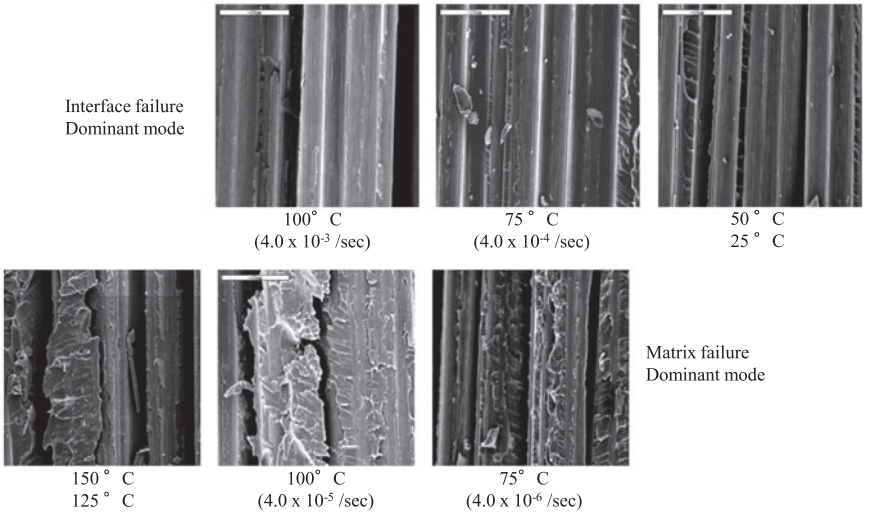

Figure 10. Failure surfaces observed by SEM. At high strain rate or low test temperature, interface-failure dominant mode appears. For opposite cases, matrix-failure dominant mode appears.[27]

specimen failed in the interface-failure dominant mode. The critical point stresses at specimen failure were calculated considering the viscoelasticity and are plotted in

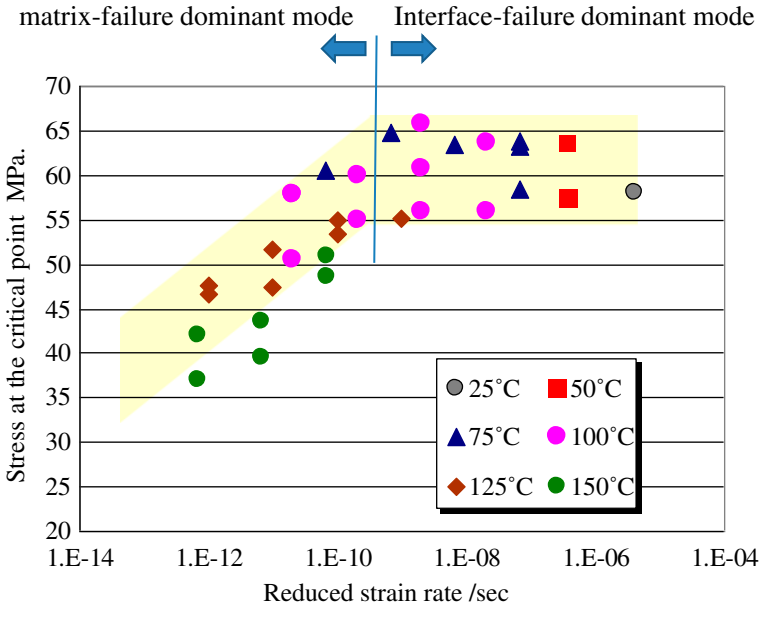

Figure 11. Critical point stress vs. reduced strain rate for various test temperature.[35] For specimen showing interface-failure dominant mode, the critical point stress is not strain-rate and temperature dependent.

Figure 11, in which the horizontal axis is the reduced strain rate. The reduced strain rate is a simulated strain rate considering the time and temperature superposition principle for high-temperature tests. As shown in the figure, the right-hand side is the interface-failure dominant mode, so the critical point stresses can be assumed to be equivalent to the interface strength. For the results, it is verified that the interface strength is time and temperature independent.[27] This conclusion is consistent with what we mentioned in the previous section.

3.2. *Periodic multi-fiber unit-cell simulation*

Indeed, a quantitative study is necessary to measure the interface strength. A more elaborate study than the above simple method is desired to be performed for that purpose. Here, we focus on the transverse failure in unidirectional composites first.

There have been numerous works on transverse failure in composite materials. Hashin [37] presented criteria in which a quadratic interaction between stress invariants on the failure plane is considered, which can be regarded as the first realistic criterion. Puck and Schurmann [38] combined the effect of internal material friction into Hashin's criteria. In addition, Davila et al. [39] proposed the LaRC03 criteria and compared the above three criteria sets with the experiments conducted in the World-Wide Failure Exercise. Totry et al. [40] compared these criteria with a numerical analysis using a periodic unit-cell (PUC) simulation, i.e. the representative volume element method. In order to simulate composite failures microscopically, they modeled individual fibers and the matrix, and they adopted the Mohr–Coulomb criterion for matrix yielding.

PUC has been the focus of many researchers over the past decade because of the relatively low computational cost; the actual modeling of all existing individual fibers within the specimen of interest is impractical in terms of the computational cost. Among these researchers, Vaughan and McCarthy [32] pointed out that both the matrix properties and interface properties affect the failure characteristics of composites. This indication is quite accurate, and so many papers dealing with interface properties exist, as mentioned in the previous section. In fact, Hobbiebrunken et al. [34] and Canal et al. [33] presented experimental evidence of interface debonding in composite failure from *in situ* observation. Romanowicz [29] and Canal et al. [30] presented composite failure simulations with cohesive zone modeling to express the interface failure. Thus, transverse failure of polymer composite materials consists of matrix failure and/or interface failure.

The following articles are worthy of special note in terms of matrix failure. Asp et al. [41] presented a scheme of critical dilatational deformation in the first quadrant of the bi-axial failure envelope for polymers, which physically suggests that cavitation or crazing occurs in polymer materials. Based on this concept, Gosse and Christensen [42] proposed a strain invariant failure theory (SIFT). SIFT agrees with the experimental results of Asp et al. [41] and was employed in the element-failure method developed by Tay et al. [43]. Canal et al. [31] also implemented a PUC simulation considering cavitation-induced brittle failure with an elasto-viscoelastic constitutive equation. The abovementioned articles deal entirely with static failure; however, the failure of a polymer matrix is usually strain rate dependent.[44–53] In order to discuss strain-rate-induced failure mode transitions from the matrix-failure dominant mode to the interface-failure dominant mode, as in Figure 10, rate-dependent matrix-failure characteristics should be taken into account; however, there have only been a few such articles.[54–58]

3.3. *Constitutive law for matrix resin*

The authors numerically simulated the characteristics of transverse failure in a unidirectional composite that depend on the strain rate.[59] We implement a PUC simulation for the failure mode transition caused by varying the applied strain rate. The unit cell consists of 20 fibers and the surrounding matrix. The fiber is assumed to be an elastic body, and the matrix is characterized by an elasto-viscoplastic constitutive equation based on damage mechanics regarding yielding and cavitation failure. As shown in Figure 12, cavitation-induced matrix failure is, in fact, observed in the cruciform specimen test, which was originally intended for the measurement of the carbon fiber/epoxy resin interfacial strength using a single-fiber composite. In the immediately neighboring fiber part, the matrix stress state is multiaxial tension, and the mean stress becomes high, which generates cavitation (void) damage. The figure shows a number of cavitations appearing with an increase in the specimen stress. For the matrix resin, it is better to model it with an elasto-viscoplastic constitutive equation that can consider cavitation-induced damage.

3.4. *Extracting interface properties from numerical analysis*

In the aforementioned article [59], the numerical implementation is based on Okabe et al. [60,61]. The parameter damage model suggested by Kobayashi et al. [62] is employed for the constitutive law in which a hardening law for ductile polymer

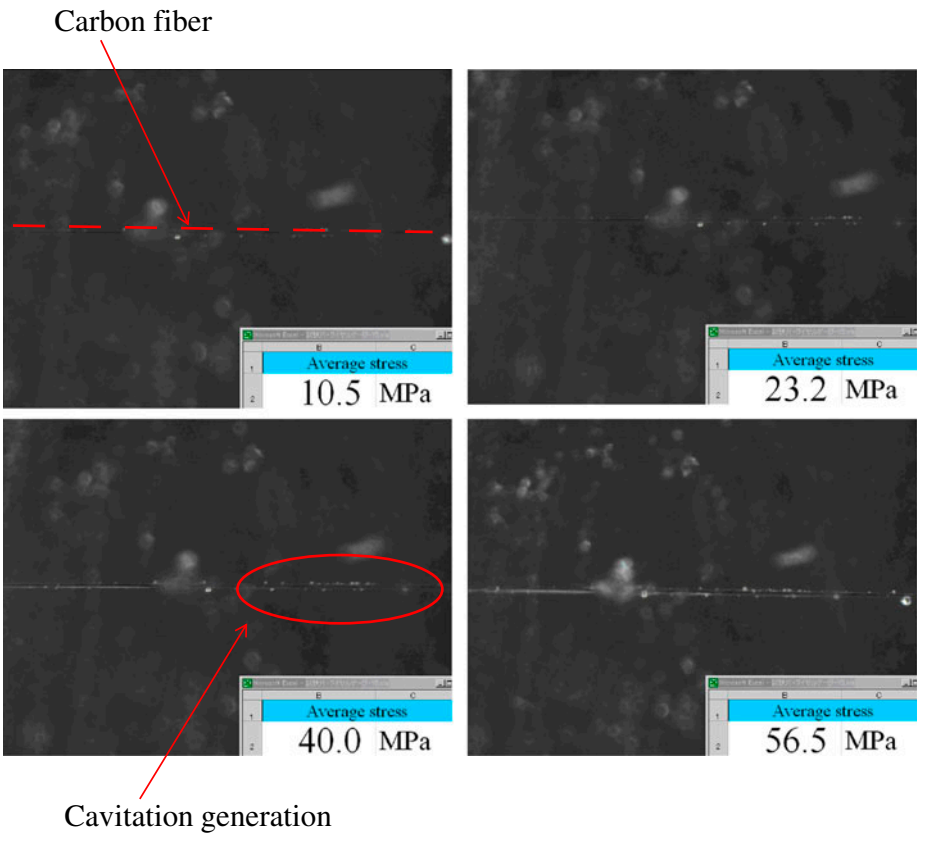

Figure 12. Magnified photographs during cruciform specimen test. Right hand side footnote is far-field stress value. Specimen consists of carbon fiber and epoxy resin. Near carbon fiber, cavitation (void) arise and increases with increase of stress.

materials [63–65] and a damage progressive law [66–69] are involved. Also, in order to eliminate the mesh dependence of the matrix damage, non-localization of the damage parameter is applied.[70,71] We performed the PUC simulation as shown in Figure 13. For interface failure, several kinds of cohesive zone modeling have been implemented in previous studies.[7,19,21,22,29–31,59] We used Dagdale-type cohesive elements, as shown in Figure 14, and considered mixed-mode interface failure.

Figure 15 shows a stress–strain curve obtained in our previous work,[59] and these results are consistent with the experimental results presented in our experimental work.[35] Figure 16 shows typical damage parameter distributions for relatively high and low strain rates and the extracted failure interface element at specimen failure. At a high strain rate, many interfaces fail (i.e. interface-failure dominant mode), and almost no interfaces fail at the low strain rate (matrix-failure dominant mode). The failure mode transition to matrix-failure dominant from interface-failure dominant with a decrease in strain rate is consistent with Figure 10. Thus, in terms of the stress–strain curves and failure mode transition, the numerical results are consistent with the experimental results only when we choose the interface properties correctly. In other words, if we take the wrong values for the interface properties, the failure mode transition does

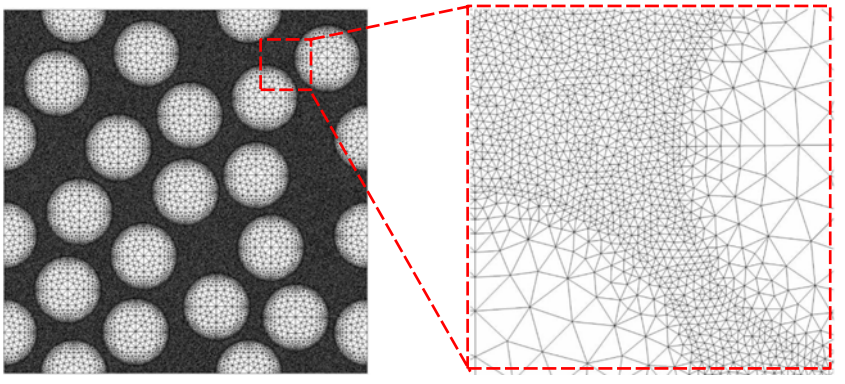

Figure 13. Periodic unit cell with mesh and magnified one: triangle quadratic element is used, fine mesh is adopted for matrix part and near interface, no volume cohesive element is inserted at every interface.[59]

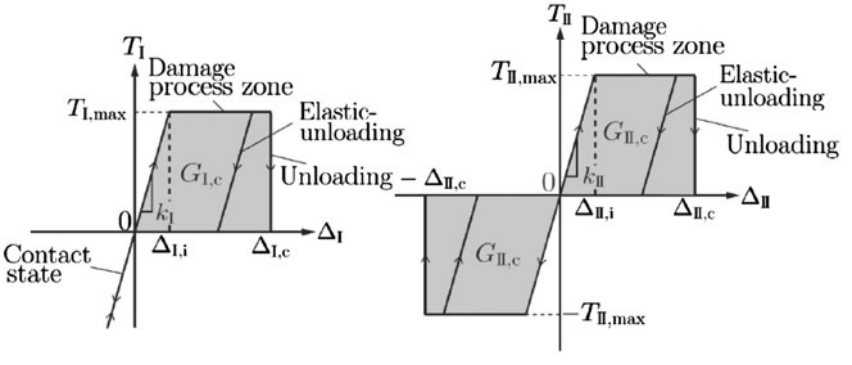

Figure 14. Traction-separation behaviors of Dagdale-type cohesive element for pure mode I and pure mode II.

not occur with a change in strain rate (i.e. there is always an interface-failure dominant mode or a matrix-failure dominant mode). As shown in Figure 17, when we set the interface strength and toughness too high or too low, failure mode transition does not occur. In this way, both the interface strength and toughness can be specified as their values should be in some range.

4. Discussions

4.1. Strength

Going back to Figure 6, no matter which interface failure criteria we use (parabolic or quadratic), the interface shear strength is higher than the interface normal strength. When the interface strength is higher than that of the matrix resin, the interface strength cannot be measured because the matrix resin fails before interface failure occurs. Hence, the interface normal strength is easier to measure. Even then, there are many cases where we cannot measure the interface strength because of earlier matrix failure,

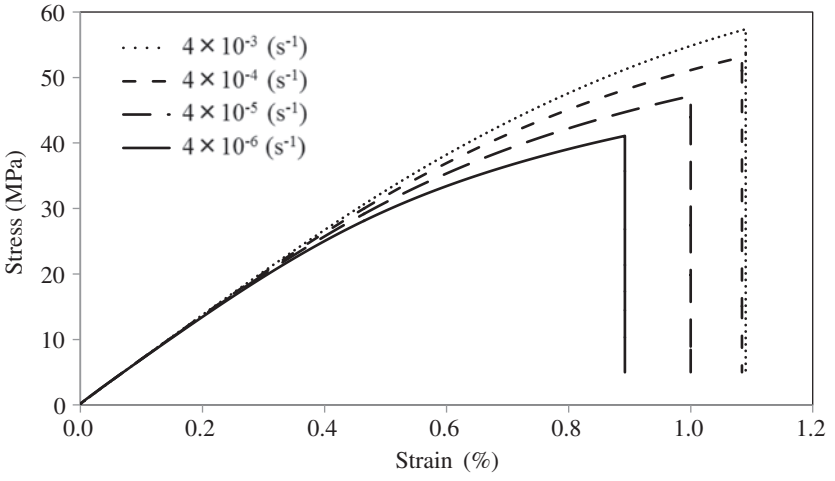

Figure 15. Stress-strain curves for various strain rates assuming 70 MPa and 1.0 N/m for interface strength and toughness, respectively.[59] Both failure stress and strain decrease with decrease in strain rate.

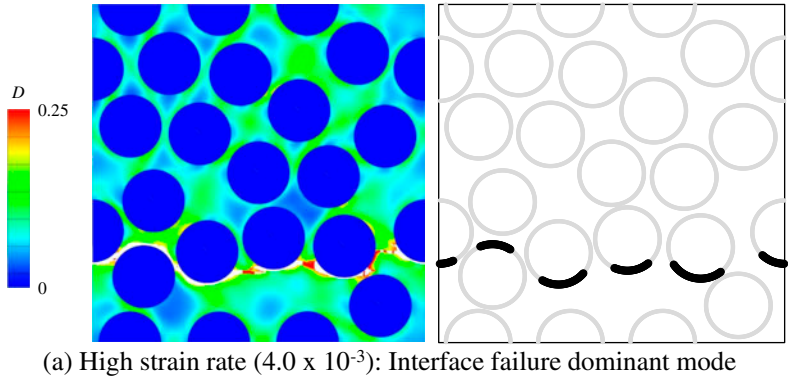

(a) High strain rate (4.0 x 10^{-3}): Interface failure dominant mode

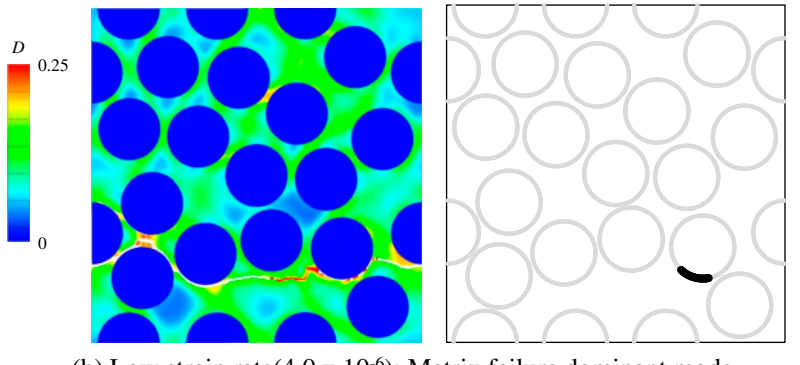

(b) Low strain rate(4.0 x 10^{-6}): Matrix failure dominant mode

Figure 16. Damage-parameter distribution and extracted interfacial debonding at ultimate failure.[59] Interface failure dominant mode occurs at high strain rate and matrix-failure dominant mode does at low strain rate, assuming $T_c = 70$ MPa, $G_c = 1.0$ N/m.

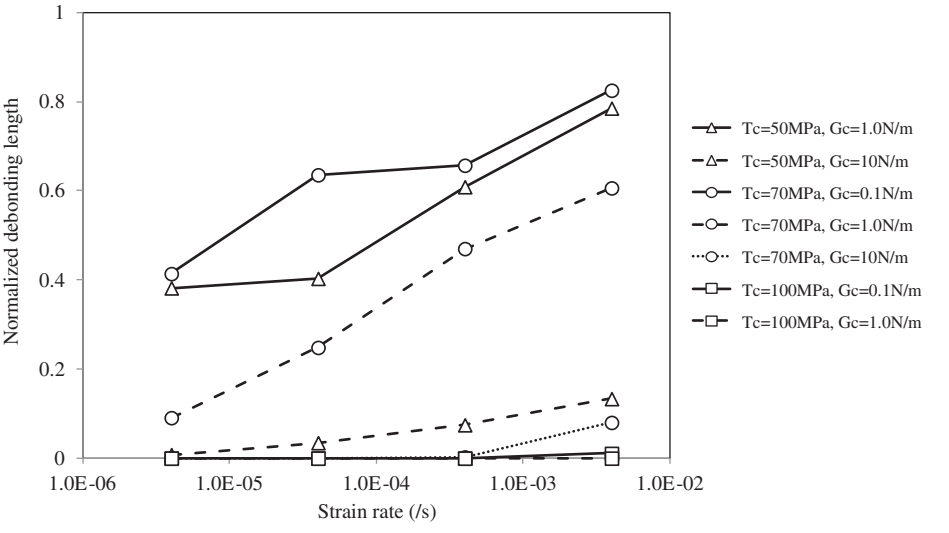

Figure 17. Relationship between debonding length normalized by unit-cell width and strain rate assuming various interface properties: $T_c = 50$, 70, 100 MPa, $G_c = 0.1$, 1.0, 10 N/m.[59] In order to simulate failure mode transition, the values of interface strength and toughness should be in some ranges.

as in the case shown in Figure 12. For such cases, there are two options that increase the measurement possibility. One is testing at a low-temperature condition, and the other is testing with a high strain rate. Both procedures are intended to simply increase the matrix resin strength. For example, using the split Hopkinson bar method in liquid nitrogen might be one of the best procedures to measure relatively high interface strengths.

On the other hand, for such cases, we do not care about interface failure when we consider composite failure. As far as we experienced, the interface of composites made of Toray carbon fiber and thermoset epoxy resin seems to be sufficiently strong. Because we hardly obtain an interface-failure dominant mode as shown in Figure 10; the appearance of an interface-failure dominant mode is, in fact, expected to be rare. This means the interface strength is at least stronger than the matrix resin even though we cannot discuss the interface strength quantitatively. However, there is the possibility that when the interface strength is too high, the composite tensile strength decreases,[1] so we might have to consider it in terms of this aspect.

4.2. *Fracture toughness of interface*

Some of the existing articles discuss the interface toughness. Among them, this paper discusses the results shown in Figures 17 and 18. Figure 17 shows the relationship between the normalized interfacial failure length (ratio of failure interface length over unit cell width) and strain rate for the transverse tensile failure of a unidirectional composite.[59] In that paper, it is concluded that the interface toughness is around 1 N/m. Figure 18 shows the relationship between the time and the interfacial debonding length in the fragmentation test, in which the far-field strain is fixed over time.[19] This paper also suggests that the interface toughness is 1 N/m because the numerical result

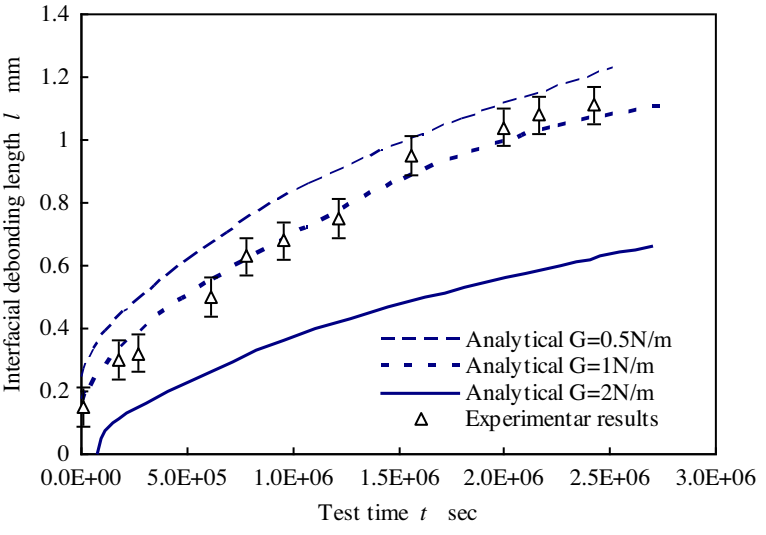

Figure 18. Comparison of analytical and experimental results of interfacial debonding length as a function of time for the time dependent interfacial failure propagation test by constant strain fragmentation test.[19]

assuming this value shows good agreement with the experimental results, whereas conventional articles present that the interface toughness is 10–200 N/m.[7,21,22,72,73] When we simulate the interface failure by cohesive zone modeling, the separation length, which indicates the interface-failure relative displacement, is limited to a small value. For instance, it is strange that the separation length is larger than the fiber radius for the case simulating interface normal failure. For this case, the matrix around the interface should fail because of the large deformation before the interface failure is recognized. It is worthy to note that the shear failure mode tests tend to provide relatively high interfacial fracture energy, and the normal failure mode tests provide low interfacial fracture energy. The actual value of the interface toughness is still currently under discussion.

4.3. Ideal interface property

At the end of this paper, we would like to describe what good interface is for continuum fiber reinforced bulk composites. We suggest the best interface strength is slightly superior to that of matrix resin because of following reason. For the composite failures in shear and compressive modes, the interface that is stronger than matrix resin does not affect on the bulk composite strengths; these strengths are dominated by the resin property for this case. Note that we assume the interface toughness is not concerned this case. On the other hand, for tensile strength of composites, a remarkably strong interface may lead composite strength reduction. There is a trade-off relationship between tensile and compressive (shear) composite strengths, controlled by the interface strength. If designers place a premium on the composite *compressive* strength, the interface strength should satisfy to be higher than matrix strength at first and then it should not be too high for the composite tensile strength; i.e., the interface that has slightly

stronger property than matrix resin is ideal for the bulk composite materials. For the meantime, the authors cannot clearly state about ideal interface toughness because its evaluation method has not been well-established as mentioned above.

5. Conclusion

This paper organizes the characteristics of interface mechanical properties for fiber-reinforced polymer matrix composites. The present paper concludes the followings aspects:

(1) When the parabolic criterion is considered for the interface failure envelope, all existing results can be reasonably explained, including its time and temperature dependence. The failure envelope is time and temperature independent, but when shear and compressive stress is applied, the interface strength looks time and temperature dependent because compressive stress changes with time and temperature, and shear strength changes simultaneously.
(2) The interface normal strength is slightly less than the interface shear strength. Therefore, the cruciform specimen test, which measures interface normal strength, is the most promising way to measure the interface strength among the micromechanical testing methods using a single-fiber composite specimen. The possibility of interfacial debonding in advance of matrix resin failure and/or yielding is more than that in shear-direction type tests.
(3) The resin meniscus should be considered in stress state analysis for single-fiber pull-out tests (including the micro-drop test). This modeling makes the stress-based failure criterion commonly applicable to various fiber-embedded lengths and even to different tests.
(4) It is possible to provide a realistic range in which the interface strength and toughness should be by comparing the PUC simulation with the experimental results in terms of failure surfaces (failure morphology), rupture stress, rupture strain, and the entire stress–strain curves.
(5) Interface toughness might be low, such as around 1 N/m. Differing from the strength discussion, the range in which the proposed interface toughness exists is still very broad. The interface toughness value suggested in the present paper is relatively low.

References

[1] Koyanagi J, Hatta H, Kotani M, Kawada H. A comprehensive model for determining tensile strengths of various unidirectional composites. J. Compos. Mater. 2009;43:1901–1914.
[2] Kim JK, Mai YW. High strength, high fracture toughness fibre composites with interface control – a review. Compos. Sci. Technol. 1991;41:333–378.
[3] Gundel DB, Majumdar BS, Miracle DB. Evaluation of the transverse response of fiber-reinforced composites using a cross-shaped sample geometry. Scripta Metall. Mater. 1995;33:2057–2065.
[4] Tandon GP, Kim RY. Fiber-matrix interfacial failure characterization using a cruciform-shaped specimen. J. Compos. Mater. 2002;36:2667–2691.
[5] Ogihara S, Koyanagi J. Investigation of combined stress state failure criterion for glass fiber/epoxy interface by the cruciform specimen method. Compos. Sci. Technol. 2010;70:143–150.
[6] Koyanagi J, Ogihara S. Temperature dependence of glass fiber/epoxy interface normal strength examined by a cruciform specimen method. Composites Part B. 2011;42:1492–1496.

[7] Koyanagi J, Shah PD,Kimura S, Ha SK¸Kawada H. Mixed-mode interfacial debonding simulation in single fiber composite under a transverse load. J Solid Mech. Mater. Eng. 2009;3:796–806.
[8] Zhandarov S, Mader E. Characterization of fiber/matrix interface strength: applicability of different tests, approaches and parameters. Compos. Sci. Technol. 2005;65:149–160.
[9] Piggott MR. Why interface testing by single-fibre methods can be misleading. Compos. Sci. Technol. 1997;57:965–974.
[10] Zhandarov SF, Pisanova EV. The local bond strength and its determination by fragmentation and pull-out tests. Compos. Sci. Technol. 1997;57:957–964.
[11] Zhou XF, Wagner HD, Nutt SR. Interfacial properties of polymer composites measured by push-out and fragmentation tests. Composites Part A. 2001;32:1543–1551.
[12] Park JM, Kim JW, Yoon DJ. Comparison of interfacial properties of electrodeposited single carbon fiber/epoxy composites using tensile and compressive fragmentation tests and acoustic emission. J. Colloid Interface Sci. 2002;247:231–245.
[13] Yang L, Thomason JL. Interface strength in glass fiber-polypropylene measured using the fibre pull-out and microbond methods. Composites Part A. 2010;41:1077–1083.
[14] Nam TH, Ogihara S, Kobayashi S. Interfacial, mechanical, and thermal properties of coir fiber-reinforced poly (lactic acid) biodegradable composites. Adv. Compos. Mater. 2012;21:103–122.
[15] Yang L, Thomason JL, Zhu W. The influence of thermo-oxidative degradation on the measured interface strength of glass fibre-polypropylene. Composites Part A. 2011;42:1293–1300.
[16] Chua PS, Piggott MR. The glass fibre – polymer interface: I – theoretical consideration for single fibre pull-out tests. Compos. Sci. Technol. 1985;22:33–42.
[17] Beckert W, Lauke B. Critical discussion of the single-fiber pull-out test: does it measure adhesion? Compos. Sci. Technol. 1997;57:1689–1706.
[18] Koyanagi J, Nakatani H, Ogihara S. Comparison of glass–epoxy interface strengths examined by cruciform specimen and single-fiber pull-out tests under combined stress state. Composites Part A. 2012;43:1819–1827.
[19] Koyanagi J, Yoshimura A, Kawada H, Aoki Y. A numerical simulation of time-dependent interface failure under shear and compressive loads in single-fiber composites. Appl. Compos. Mater. 2010;17:31–41.
[20] Straub A, Slivka M, Schwartz P. A study of the effects of time and temperature on the fiber/matrix interface strength using the microbond test. Compos. Sci. Technol. 1997;57:991–994.
[21] Nishikawa M, Okabe T, Hemmi K, Takeda N. Micromechanical modeling of the microbond test to quantify the interfacial properties of fiber-reinforced composites. Int. J. Solids Struct. 2008;45:4098–4113.
[22] Nishikawa M, Okabe T, Takeda N. Determination of interface properties from experiments on the fragmentation process in single-fiber composites. Mater. Sci. Eng., A. 2008;480:549–557.
[23] Tripathi D, Jones FR. Single fibre fragmentation test for assessing adhesion in fibre reinforced composites. J. Mat. Sci. Eng. 1998;33:1–16.
[24] Kim JK, Baillie C, Mai YW. Interfacial debonding and fibre pull-out stresses. J. Mater. Sci. 1991;27:3143–3154.
[25] Herrera-Franco PJ, Drzal LT. Comparison of methods for the measurement of fibre/matrix adhesion in composites. Composites. 1992;23:2–27.
[26] Piggott MR. Debonding and friction at fibre-polymer interfaces. I: Criteria for failure and sliding. Compos. Sci. Technol. 1987;30:295–306.
[27] Koyanagi J, Yoneyama S, Nemoto A, Melo J. Time and temperature dependence of carbon/epoxy interface strength. Compos. Sci. Technol. 2010;70:1395–1400.
[28] Ha S, Jin K, Huang Y. Micro-mechanics of failure (MMF) for continuous fiber reinforced composites. J. Compos. Mater. 2008;42:1873–1895.
[29] Romanowicz M. Progressive failure analysis of unidirectional fiber-reinforced polymers with inhomogeneous interphase and randomly distributed fibers under transverse tensile loading. Composites Part A. 2010;41:1829–1838.
[30] Canal LP, Segurado J, LLorca J, Filure J. Failure surface of epoxy-modified fiber-reinforced composites under transverse tension and out-of-plane shear. Int. J. Solids Struct. 2009;46:2265–2274.
[31] Canal LP, Segurado J, LLorca J. Failure surface of epoxy-modified fiber-reinforced composites under transverse tension and out-of-plane shear. Int. J. Solids Struct. 2009;46:2265–2274.

[32] Vaughan TJ, McCarthy CT. Micromechanical modelling of the transverse damage behaviour in fibre reinforced composites. Compos. Sci. Technol. 2011;71:388–396.
[33] Canal LP, González C, Segurado J, LLorca J. Intraply fracture of fiber-reinforced composites: microscopic mechanisms and modeling. Compos. Sci. Technol. 2012;72:1223–1232.
[34] Hobbiebrunken T, Hojo M, Adachi T, Jong CD, Fiedler B. Evaluation of interfacial strength in CF/Epoxies using FEM and in-situ experiments. Composites Part A. 2006;37:2248–2256.
[35] Koyanagi J, Yoneyama S, Eri K, Shah P. Time dependency of carbon/epoxy interface strength. Compos. Struct. 2010;92:150–154.
[36] Ramberg W, Osgood WR. Description of stress-strain curves by three parameters. Technical Note No. 902. Notional Advisory Committee on Aeronautics (NACA); 1943. Available from: https://archive.org/details/nasa_techdoc_19930081614
[37] Hashin Z. Failure criteria for unidirectional fiber composites. J. Appl. Mech. 1980;47:329–334.
[38] Puck A, Schürmann H. Failure analysis of FRP laminates by means of physically based phenomenological models. Compos. Sci. Technol. 2002;62:1633–1662.
[39] Davila CG, Camanho PP, Rose CA. Failure criteria for FRP laminates. J. Compos. Mater. 2005;39:323–345.
[40] Totry E, González C, LLorca J. Failure locus of fiber-reinforced composites under transverse compression and out-of-plane shear. Compos. Sci. Technol. 2008;68:829–839.
[41] Asp LE, Berglund LA, Talreja R. Prediction of matrix-initiated transverse failure in polymer composites. Compos. Sci. Technol. 1996;56:1089–1097.
[42] Gosse JH, Christensen S. Strain invariant failure criteria for polymers in composite materials. AIAA. 2001;A01-25005:1184.
[43] Tay TE, Tan SHN, Tan VBC, Gosse JH. Damage progression by the element-failure method (EFM) and strain invariant failure theory (SIFT). Compos. Sci. Technol. 2005;65:935–944.
[44] Guedes RM. Analysis of a delayed fracture criterion for lifetime prediction of viscoelastic polymer materials. Mech. Time-Depend. Mater. 2012;16:307–316.
[45] Melo JD, Medeiros AM. Long-term creep rupture failure envelope of epoxy. Mech. Time-Depend. Mater. Forthcoming.
[46] Bai Y, Keller T, Vallée T. Modeling of stiffness of FRP composites under elevated and high temperatures. Compos. Sci. Technol. 2008;68:3099–3106.
[47] Fritzen F, Böhlke T. Reduced basis homogenization of viscoelastic composites. Compos. Sci. Technol. 2013:84–91.
[48] Zupancic B, Emri I. Time-dependent constitutive modeling of drive belts – II. The effect of the shape of material retardation spectrum on the strain accumulation process. Mech. Time-Depend. Mater. 2009;13:375–400.
[49] Khan KA, Muliana AH. Fully coupled heat conduction and deformation analyses of viscoelastic solids. Mech. Time-Depend. Mater. 2012;16:461–489.
[50] Hirsekorn M, Petitjean F, Deramecourt A. A semi-analytical integration method for the numerical simulation of nonlinear visco-elasto-plastic materials. Mech. Time-Depend. Mater. 2011;15:139–167.
[51] Carniel EL, Fontanella CG, Stefanini C, Natali AN. A procedure for the computational investigation of stress-relaxation phenomena. Mech. Time-Depend. Mater. 2013;17:25–38.
[52] Pawlikowski M. Non-linear approach in visco-hyperelastic constitutive modelling of polyurethane nanocomposite. Mech. Time-Depend. Mater. Forthcoming.
[53] Sorvari J, Hämäläinen J. Time integration in linear viscoelasticity – a comparative study. Mech. Time-Depend. Mater. 2010;14:307–328.
[54] Raimondo L, Iannucci L, Robinson P, Curtis PT. Modelling of strain rate effects on matrix dominated elastic and failure properties of unidirectional fibre-reinforced polymer–matrix composites. Compos. Sci. Technol. 2012;72:819–827.
[55] Kontou E, Kallimanis A. Thermo-visco-plastic behaviour of fibre-reinforced polymer composites. Compos. Sci. Technol. 2006;66:1588–1596.
[56] Tabiei A, Aminjikarai SB. A strain-rate dependent micro-mechanical model with progressive post-failure behavior for predicting impact response of unidirectional composite laminates. Compos. Struct. 2009;88:65–82.
[57] Jendli Z, Fitoussi J, Meraghni F, Baptiste D. Anisotropic strain rate effects on the fibre–matrix interface decohesion in sheet moulding compound composites. Compos. Sci. Technol. 2005;65:387–393.

[58] Seelig T. Computational modeling of deformation mechanisms and failure in thermoplastic multilayer composites. Compos. Sci. Technol. 2008;68:1198–1208.
[59] Koyanagi Jun, Sato Yukihiro, Sasayama Toshiki, Okabe Tomonaga, Yoneyama Satoru. Numerical simulation of strain-rate dependent transition of transverse tensile failure mode in fiber-reinforced composites. Composites Part A. 2014;56:136–142.
[60] Okabe T, Nishikawa M, Toyoshima H. A periodic unit-cell simulation of fiber arrangement dependence on the transverse tensile failure in unidirectional carbon fiber reinforced composites. Int. J. Solids Struct. 2011;48:2948–2959.
[61] Okabe T, Motani T, Nishikawa M, Hashimoto M. Numerical simulation of microscopic damage and strength of fiber-reinforced plastic composites. Adv. Compos. Mater. 2012;21:147–163.
[62] Kobayashi S, Tomii D, Shizawa K. A modelling and simulation on failure prediction of ductile polymer based on craze evolution and annihilation. Trans. Jpn. Soc. Mech. Eng. Ser. A. 2004;70:810–817.
[63] Matsuda T, Ohno N, Tanaka H, Shimizu T. Homogenized in-plane elastic-viscoplastic behavior of long fiber-reinforced composites. JSME Int. J. Ser. A. 2002;45:538–544.
[64] Jeong HY. A new yield function and a hydrostatic stress-controlled void nucleation model for porous solids with pressure-sensitive matrices. Int. J. Solids Struct. 2002;39:1385–1403.
[65] Zhou Y, Akanda SR, Jeelani S, Lacy TT. Nonlinear constitutive equation for vapor-grown carbon nanofiber-reinforced SC-15 epoxy at different strain rate. Mater. Sci. Eng., A. 2007;465:238–246.
[66] Fiedler B, Hojo M, Ochiai S, Schulte K, Ando M. Failure behavior of an epoxy matrix under different kinds of static loading. Compos. Sci. Technol. 2001;61:1615–1624.
[67] Nishikawa M. Multiscale modeling for the microscopic damage and fracture of fiber-reinforced plastic composites [Dr Eng. thesis]. Tokyo: The University of Tokyo; 2008 (in Japanese).
[68] Gurson AL. Continuum theory of ductile rupture by void nucleation and growth, Part I, yield criteria and flow rules for porous ductile media. Trans ASME, J. Eng. Mater. Technol. 1977;99:2–15.
[69] Tvergaard V, Needleman A. Analysis of the cup-cone fracture in a round tensile bar. Acta Metall. 1984;32:157–169.
[70] Tvergaard V, Needleman A. Effects of nonlocal damage in porous plastic solids. Int. J. Solids Struct. 1995;32:1063–1077.
[71] Pijaudier-Cabot G. Nonlocal damage theory. J. Eng. Mech. 1987;113:1512–1533.
[72] Yuan MN, Yang YQ, Xia ZH. Modeling of push-out test for interfacial fracture toughness of fiber-reinforced composites. Adv. Compos. Mater. 2012;21:401–412.
[73] Kimura S, Koyanagi J, Kawada H. Evaluation of initiation of the interfacial debonding in single fiber composite (energy balance method considering an energy dissipation of the plastic deformation). JSME Int. J. Ser. A. 2006;49:451–457.